MEASURE OF THE SOLAR FLUX CONVEYED ONTO A LAMBERTIAN TARGET BY A NOVEL BI-AXIAL FRESNEL CONCENTRATOR

Marco Antonelli Gianluca Caposciutti

University of Pisa, Department of Energy, Systems, Territory and Constructions (D.E.S.Te.C.)

ABSTRACT

This paper deals with the optical analysis of a prototype of a novel concentrator, named as Bi-Axial Fresnel (BAF). This concentrator aims at reducing production and installation costs, as well as keeping as low as possible the weight and the bulk of the mirrors field, making it suitable for building small-dimensions systems, able to be placed on industrial roofs, as an example. The prototype is composed as an array of 3x3 mirrors. Its theoretical concentration is therefore 9. The experiment made use of a very basic equipment, which included a thermal flux sensor and a simple webcam, properly equipped for distinguish grey scales under quite high solar intensities. The concentrator was governed by an Arduino card, while the acquisition took place by means of a National Instruments acquisition board and Labview software. The aim of this experimental setup was the reconstruction of the solar flux on a fixed Lambertian target, based on the grey-scale maps gathered through the webcam and properly scaled accordingly to the punctual solar flux measured by the sensor. This way, the experimental apparatus was able to get an estimation of the solar power conveyed to the target.

NOMENCLATURE

Put nomenclature here.

INTRODUCTION

In Concentrated Solar Power, the advantages in concentrating a high solar radiation flux on a very small area receiver inducing high temperature operations is an effective mean for reducing heat losses and achieving high conversion efficiency [1, 2]. Concentrator types differentiate each other depending on the solar concentration ratio, which establishes the power density of concentrated sunlight. Currently, five CSP technologies exist, classified in increasing order of concentration ratio: Compound Parabolic Collectors [3, 4], Parabolic-Through Collectors, Linear Fresnel Collectors, Solar Tower Power, and Parabolic Dish Collectors [5, 6]. High concentration systems are often used to drive a gas turbine, in which the solar receiver replaces or integrates the combustion chamber. As concentration increases, however, more and more precise tracking is required and the dimensions of the optical system (mirror or lens) increases. These systems, in short, are expensive and practically impossible to be placed on surfaces such as roofs and coverings. Large free portions of soil are therefore required for their location. From this point of view, the linear Fresnel reflector is to be preferred to the others, since the mirrors are flat and very narrow in cross section and due to their shape and location, they are less subject to actions by the wind and other atmospheric agents and, thanks to a lighter structure, they can be installed on industrial and residential roofs. However, the low concentration does not generally allow a receiver to surpass temperatures >250 °C.

The novel bi-axial Fresnel (BAF) concentrator is a two-axes concentrator based on the use of flat or slightly curved mirrors. The concentrator is constituted by an array of strings, each one carrying a plurality of mirrors, which can be rotated along an axis in a coordinated manner by means of a mechanical linkage. A bi-axial movement is then achieved by means of the movement of the mirrors along two perpendicular axes, with a much-reduced number of servomotors with respect to a conventional bi-axial concentrator, which usually requires two motors per mirror. The concentration ratio is roughly the square of a conventional single-axis Fresnel, thereby allowing a higher operating temperature.

The present work deals with an innovative model of solar concentrator based on the Fresnel spotlight concept. This plant technology is well consolidated for large size plants [7], but for small size plants it shows losses at extremities that are relevant [8]. A point-based concentration system was therefore developed, rather than linear and moving on two axes instead of on one axis only.

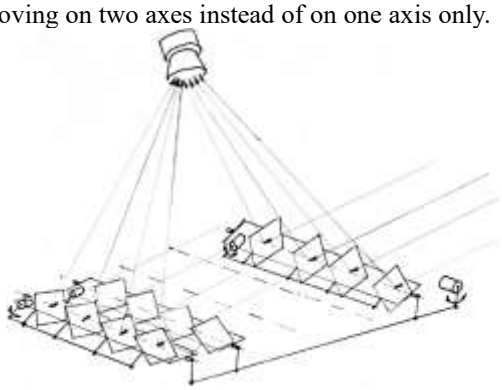

Figure 1. Concept of the Bi-Axial Fresnel (BAF)

In the configuration analyzed in this work, the rows of mirrors, by means of a crank mechanism, are moved, synchronously, by a single servomotor. This synchronous movement also takes place between the

mirrors of each single row, where there is a crank mechanism operated by a single servomotor. The target receiver is positioned on the top of the machine and has the function of collecting the radiation as well conveyed and concentrated, remaining rigidly bound to the structure. The two axes of the system, around which the optical elements and each articulated frame move, can be oriented in any way with respect to the apparent motion of the Sun with respect to the Earth.

METHOD

An experimental model of the object of study described above has been realized, which is visible in Figure 2. This system is composed of 9 square-shaped aluminum flat mirrors, which reflect light on an opaque white target, also square and equipped with a system for measuring the collected radiation. The theoretical concentration of this device is therefore 9.

Figure 2. Lab-scale prototype of the BAF concentrator

The experimental apparatus is therefore divided into:

1. A stand-alone system to carry out solar tracking and the pointing of mirrors on the target, where an Arduino Nano microcontroller continuously controls the positioning of the mirrors through data collected by a solar tracker positioned above the field of mirrors. The tracker (figure 3) consists of two servomotors and four photoresistors for alignment with the solar direction and allows the estimation of the altitudinal and azimuthal angles of the Sun. When all the four photoresistors provide the same reading, the tracker is aligned with the solar rays.
2. A computer-controlled system, which allows to acquire the value of the incident solar radiation on the target through a thermal flux sensor. In addition, the radiation reflected on the target is continuously monitored through a webcam and appropriate filters to reduce the light intensity, compatibly with the sensitivity of the device (Figure 4).

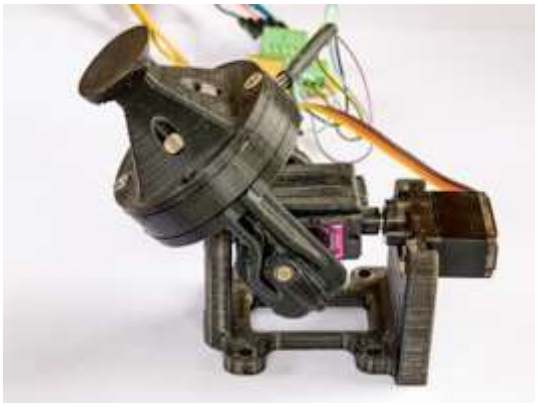

Figure 3. Solar tracker

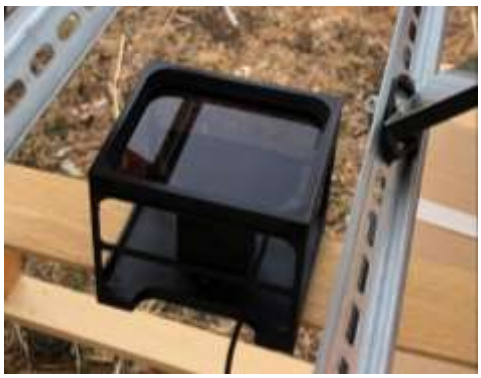

Figure 4. Webcam with attenuation grey filters

The kinematics for the movement of mirrors is visible in Figure 5. This kinematics provides that the reflectors are moved on two axes orthogonal to each other, where the 3 rows of mirrors (each of which contains 3 other mirrors) are moved synchronously, through a crank, by a single servo motor.

Figure 5. Focus on the moving frames and mirrors

The individual mirrors, on the other hand, move synchronously by rotating around their side pins thanks to three servomotors that receive the same adjustments from the control system. The reciprocal position of frames and mirrors can be adjusted by means of verniers (Figures 6 and 7).

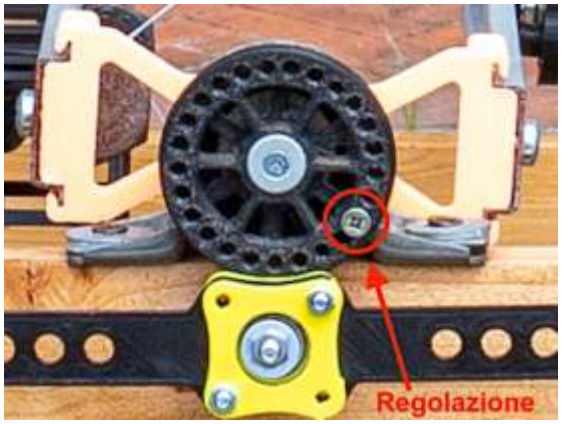

Figure 6. Frame initial position adjustment system

Figure 7. Mirrors'initial position adjustment system

The instrumentation of the data acquisition system consists of an Arduino Uno microcontroller, a webcam, a National Instruments voltage analog signal acquisition board, a heat flow sensor, a signal converter, a servo motor.

The programming of the system for solar concentration took place in the Arduino integrated development environment in such a way as to exploit the signals sent by the four photoresistors installed on the tracker to perform the solar tracking. The program thus detects the angular positions of the tracker and performs calculations to derive the angles of movement of the mirrors to concentrate the solar radiation on the target, as reported in the block diagram of Figure 7.

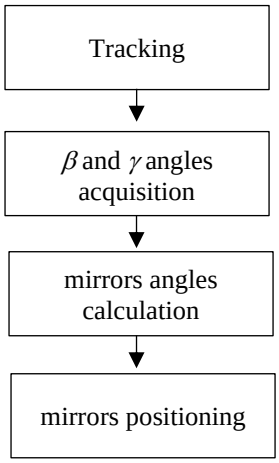

Figure 8. Characteristic angles of the system

The calculation of the angles of movement of the mirrors was performed based on the angular relations that refer to the diagram in Figure 8.

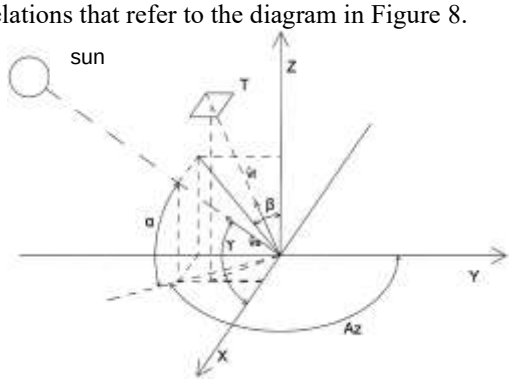

Figure 9. Characteristic angles of the system

Where β and γ are the angles assumed by the solar tracker. Similarly, θ and ϕ are also defined, which are angles homologous to β and α defines the solar height and the angle A_z is the azimuth angle. Since all mirrors move synchronously and receive the same adjustments from the control system, the calculations refer only to the central mirror.

Once the solar tracker gathers the angles β and γ, it is possible to calculate the sun-mirror versor v_s. Since the target mirror versor v_t is also known, it is possible to calculate the vector normal to the surface of the mirrors, which will coincide with the bisector of the angle between v_s and v_t. Normalizing this vector allows to calculate the angles θ and ϕ by means of trigonometric relations applied to its components.

It is also possible to derive the relationships between β and γ and the solar coordinates α and A_z. The following Equations 1 and 2 define the angles of the mirrors θ and ϕ and the theoretical angles β and γ, respectively.

$$\begin{cases} \phi = arccos\left(\frac{v_{sx}+v_{rx}}{|v_n|}\right) \\ \theta = arccos\left(\frac{v_{nz}}{sin\phi \cdot |v_n|}\right) \end{cases} \quad (1)$$

$$\begin{cases} \gamma = \arccos\left(\cos(\alpha)\cdot\cos(A_z - 90)\right) \\ \beta = arctan\left[\frac{\cos(\alpha)\cdot\sin(A_z-90)}{\sin(\alpha)}\right] \end{cases} \quad (2)$$

The code, during the processing phase of the corners of the mirrors, therefore, performs the following operations:

1. gathers β and γ, from the solar tracker,
2. calculates v_{sx}, v_{sy} and v_{sz}, which are the components of the mirror Sun versor,
3. the target-mirrors versor is known since it is fixed by construction and so are its components v_{tx}, v_{ty} and v_{tz} are,
4. calculates $v_{sx} + v_{tx}$, $v_{sy} + v_{ty}$ and $v_{sz} + v_{tz}$,
5. calculates $|\vec{v}_n|$, which is the modulus of the versor normal to the surface of the mirror, and its components v_{nx}, v_{ny} and v_{nz},,

6. calculates θ and ϕ.

The acquisition system tasks instead are measuring the thermal flux in the central point of the target and grabbing the image of the target itself as grayscale picture. The tasks of this Labview program therefore are acquiring the measurement of the heat flux sensor placed in the center of the target and the photograph of the target, controlling the exposure system of the sensor, and continuously acquiring the angular position of the two servomotors that move the solar tracker. The thermal flux sensor was a Hukseflux SBG01, with a rated measurement range of 10 kW/m^2 (Figure 10).

Figure 10. Thermal flux sensor Hukseflux SBG01

The picture of the target is acquiring after having closed the orifice by means of a moving scoop, painted with the same color of the target (figure 11). Since the thermal flux sensor has quite a long time constant, the target picture was acquired after the thermal flux reading. All this process took place every two minutes.

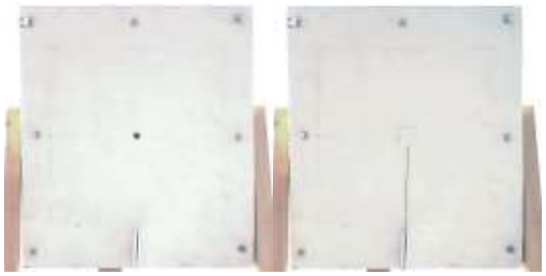

Figure 11. Target with open (left) and closed (right) orifice

This code first realizes in an exact crop of the target framed by the photo, then performs three different types of conversions:

1. black and white via the im2bw algorithm,
2. grayscale using the rgb2gray algorithm,
3. color map corresponding to the distribution of heat flux on the surface of the target.

An example of these three conversions is shown in Figure 13. The first image, (in black and white) is useful to evaluate the optical performance of the concentration, the other (color map) instead shows an estimate of the distribution of the thermal flow on the target and is therefore useful to evaluate the efficiency of the system. The scaling factor between grayscale and actual flux was calculated by the comparing the thermal flux detected by the sensor and the gray intensity measured on the moving scoop. The latter was derived from the grayscale and the measurement of the heat flow sensor located in the center of the target. By assigning the value measured by the sensor to the central point of the grayscale image and thus scaling all other values of that scale, an estimate of the heat flux distribution in W/m^2 over the entire surface of the target is obtained.

The result of this conversion with a scale in W/m^2 is reported in Figure 13.

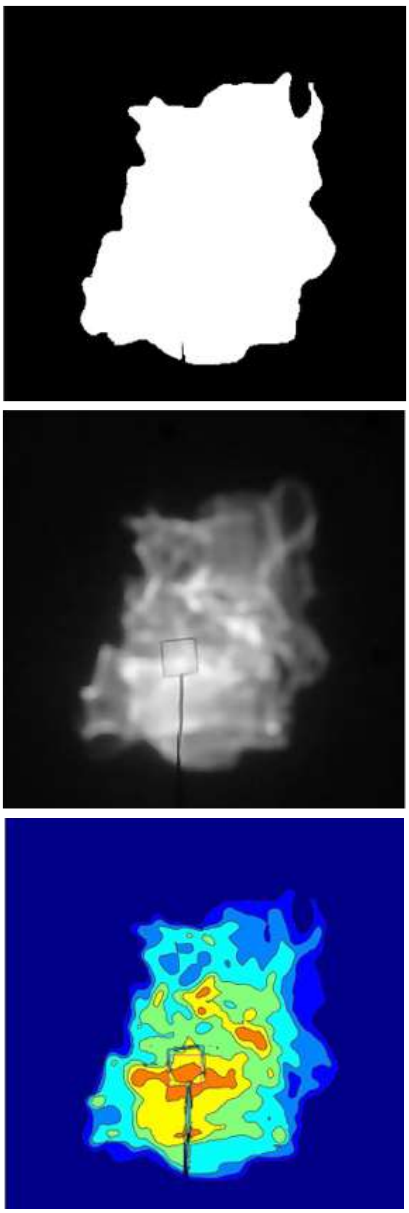

Figure 12. Three-step elaboration procedure

The data processed in the three different days can be compared using indicators.

Indicator 1 is dimensionless defines the ratio of illuminated area A_i to target area A_t and is expressed by Equation 3:

$$I_1 = \frac{A_i}{A_t} \qquad (3)$$

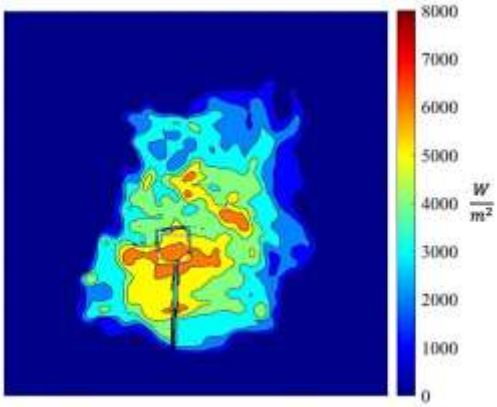

Figure 13. Example of conversion into colourmap

Indicator 2 is expressed in W/m^2 and it is the average value of the solar flux incident onto the target, calculated on the basis of the grayscale maps (Figure 9, middle).

Indicator 3 has size W and defines the average integral power of the radiation flux over the entire target. It is defined by the following Equation 4:

$$I_3 = \frac{\int I \, dA_t}{N_m \cdot A_m \cdot I_s} \quad (4)$$

Where:

1. A_t is the target area.
2. A_m is the mirror area.
3. N_m is the mirror number
4. I is the radiation on the target reconstructed on the basis of the grayscale map.
5. I_s is the sun irradiation normal to the mirrors and it was calculated from the total value of the radiation I_{ng} normal to the ground, obtained from the DESTeC weather station. I_s was therefore calculated as a function of the time and inclination of the mirror as in equation 5:

$$I_s = \frac{I_{ng}}{\cos(\theta) \cdot \sin(\phi)} \quad (5)$$

RESULTS AND DISCUSSION

At first, the correctness of operation was checked by verifying the correct positioning of the solar tracker. The angles detected by the solar tracker were compared (Figure 14) with those calculated on the basis of the day, the hour and the geographical coordinates [3].

The trend of the real angles showed to substantially agree with the theoretical angles and the deviations may depend on disturbing effects such as cloudiness or reflection of light radiation caused by parked cars and the adjacent wall.

For an optical verification of the system, on the other hand, it is necessary to observe the trend of indicator 1, (Figure 15).

Ideally, this indicator should have a constant trend throughout the day because the best possible pointing condition should always be maintained, which corresponds to the initial setting. Instead, the peak occurs at the maximum value assumed by the angle γ (defined as a function of the solar coordinates and the orientation of the machine), or when the mirrors' position is more vertical. Under these conditions the angle between incident and reflected rays is the maximum and the illuminated target area grows. In addition, this effect is influenced by the imperfections of the reflective surface of the mirrors, which is not perfectly flat and therefore alters the angle of reflection.

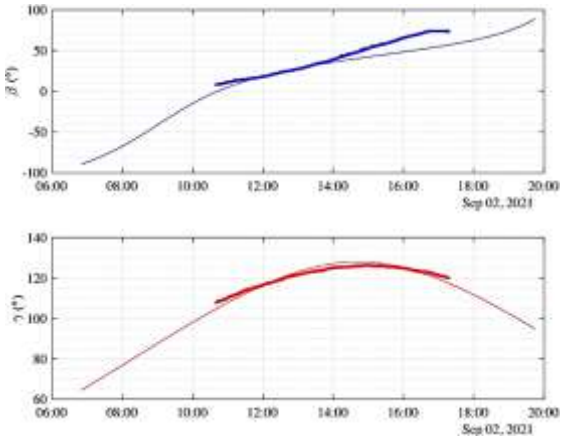

Figure 14. Comparison between the solar angles detected by the tracker (blue and red lines) and calculated on the basis of hour, day and geographical coordinates

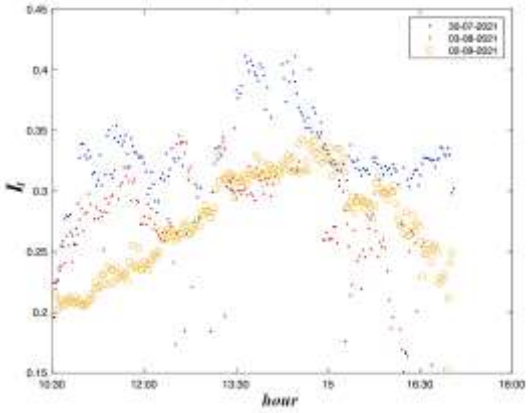

Figure 15. Trend of Indicator n. 1 as a function of the hour

Indicators 2 and 3, as expected, depend on the intensity of solar radiation, on the angles of the mirrors (and therefore also by the solar coordinates) and on the orientation of the machine since the maximum occurs around 3 pm. As expected, indicator 1 also has a maximum that occurs in the usual time slot and has a similar trend to that of indicators 2 and 3.

The average value of the irradiance (indicator n. 2) on the target was far lower than expected, since it had a maximum of about 2000 W/m2, which was quite low if compared with the theoretical value (Figure 16).

The sun irradiance in facts was about 800 W/m^2 (figure 17), which, if multiplied by the theoretical concentration, gives 7200 W/m^2. This poor

performance is to be mainly attributed to the imperfection in the mirrors' construction (poor planarity) and to the relatively high backlash in the mirrors and frames linkages. This fact is witnessed (as an example) by Figure 10, which shows that the shape of the illuminated area is far from a square and a lot of sun rays are dispersed on a relatively wide area on the target. In addition, the proportionality between gray intensity and solar flux is to be more accurately checked.

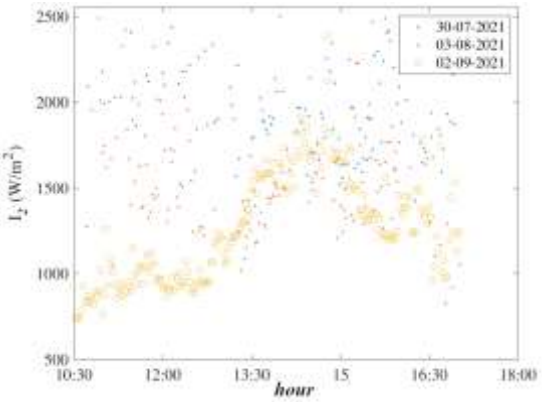

Figure 16. Indicator n. 2 trend as a function of the hour

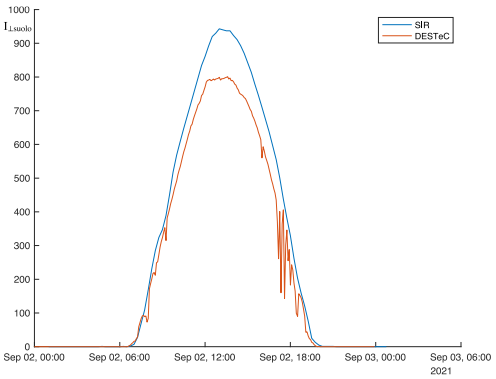

Figure 17. Sun irradiance normal to the ground

Indicator n. 3 (Figure 18) showed the same trend than indicator n. 2. This indicator represents the useful amount of solar energy conveyed on the target and its value is roughly one third than expected, similarly to indicator n. 2. The same considerations can be applied, too.

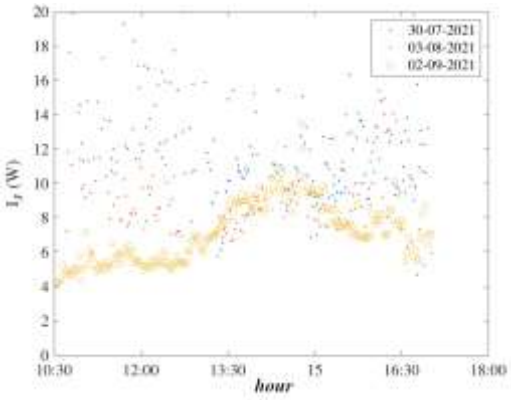

Figure 18. Indicator n. 3 trend as a function of the hour

CONCLUSIONS

An experimental model of a biaxial Fresnel-type concentrator was created, of which the control system was developed, and an instrumentation useful for making measurements and comparisons about the optical and mechanical efficiency of the entire system was added. Through these measurements, carried out through a webcam and a heat flow sensor, an estimate of the thermal flow on the surface of the target was obtained in the form of a color map. Some indicators of the concentrator's performance were also developed, which pointed out its correct functioning.

This work represents a first verification of the functionality of the system, which offers possibilities for improvement, among these we can list:

1. a refinement of the mechanics of actuation of the movement of columns and mirrors,
2. an improvement in the realization of mirrors (flatness),
3. the realization of the device with materials and methodologies suitable for continuous exposure to atmospheric agents,
4. the implementation of a camera for scientific use,
5. a more precise analysis of the correspondence between the intensity of gray detected by the camera and the actual intensity of the light incident on the target.

REFERENCES

[1] Goswami Y., Energy: the burning issue, Refocus (January–February), Elsevier, 2007, pp. 22-25.
[2] Goswami Y., Kreith F., Energy efficiency and renewable energy, Second edition, CRC Press, 2016.
[3] https://globalsolaratlas.info/map, 4 Agosto 2021.
[4] Kalogirou S., Solar energy engineering, Academic Press, 2009, pp. 49-60.
[5] Duffie J., Beckman W., Solar engineering of thermal processes, Fourth edition, John Wiley & Sons, 2013.
[6] Muhammad I., An introduction to solar radiation, Academic Press, 1983.
[7] Trucchi D., Bellucci A., Girolami M., et al., Solar Thermionic-Thermoelectric Generator (ST2G): Concept, Materials, Engineering, and Prototype Demonstration, Advanced Energy Materials, Wiley-VHC Verlag GmbH & Co. KGaA, 2018.
[8] Rubini L., Habib G., Lavra M., Tecnologie solari a concentrazione - produzione di calore a media temperatura, Report Ricerca di Sistema Elettrico, Enea, 2011.